ACTA GEOGRAPHICA SLOVENICA

GEOGRAFSKI ZBORNIK

2025
65
2

Acta geographica Slovenica, 65-2, 2025, 65–89

SPATIOTEMPORAL ANALYSIS OF LIGHT POLLUTION IN SAMSUN (TURKEY) USING SPATIAL STATISTICS AND ALGEBRA FROM SNPP/VIIRS SATELLITE IMAGERY

Sarp Doruk Ozturk, Derya Ozturk

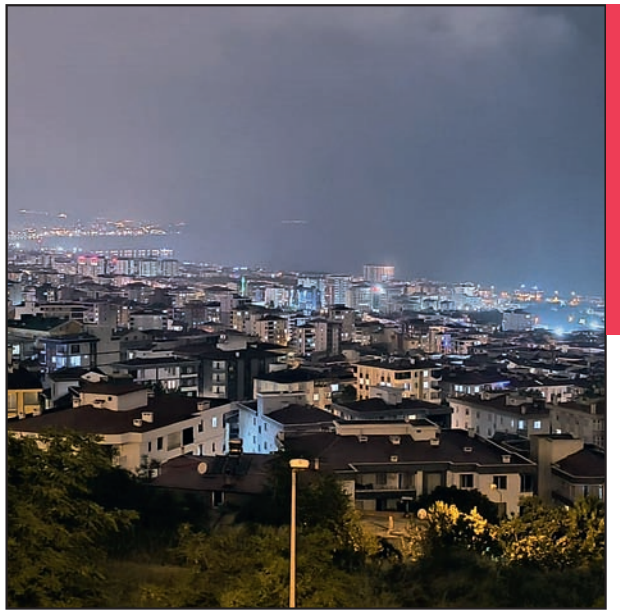

SARP DORUK OZTURK

Nighttime urban glow illustrating the extent of light pollution in Samsun, Turkey.

DOI: https://doi.org/10.3986/AGS.14506
UDC: 504.6:628.971.7(560Samsun)"2012/2024"
528.8(560Samsun)"2012/2024"

Sarp Doruk Ozturk[1], Derya Ozturk[2]

Spatiotemporal analysis of light pollution in Samsun (Turkey) using spatial statistics and algebra from SNPP/VIIRS satellite imagery

ABSTRACT: This study analyzes the spatiotemporal changes in light pollution in Samsun (Turkey) from 2012 to 2024 using remote sensing and geographic information systems. SNPP/VIIRS satellite data from five years were examined using spatial statistics and algebraic methods to measure nighttime light variations. Results show a sharp decline in dark sky areas and expansion of high light zones from 85.9 km² to 139.5 km², and medium zones from 87.6 km² to 145.5 km², driven by urbanization and industrial growth. Rapid changes occurred in Atakum, Ilkadim, Canik, and Tekkekoy, affecting sensitive ecological and astronomical sites. The strong correlation between light emissions and socio-economic indicators highlights the need for sustainable lighting policies to mitigate adverse environmental impacts.

KEYWORDS: light pollution, remote sensing, geographic information systems, spatiotemporal analysis, SNPP/VIIRS, urbanization, environmental sustainability

Prostorsko-časovna analiza svetlobnega onesnaženja v Samsunu (Turčija) z uporabo prostorske statistike in algebre na podlagi satelitskih posnetkov SNPP/VIIRS

POVZETEK: Članek na podlagi daljinskega zaznavanja in geografskih informacijskih sistemov analizira prostorsko-časovne spremembe svetlobnega onesnaženja v turškem mestu Samsun med letoma 2012 in 2024. Za merjenje sprememb nočne svetlobe so bili na podlagi prostorske statistike in algebrskih metod preučeni satelitski podatki SNPP/VIIRS za pet let. Rezultati kažejo izrazito krčenje območij temnega neba ter širitev površine močno osvetljenih območij s 85,9 km² na 139,5 km² in srednje osvetljenih območij z 87,6 km² na 145,5 km², kar je posledica urbanizacije in industrijske rasti. Najhitrejše spremembe so bile zabeležene v četrtih Atakum, Ilkadim, Canik in Tekkekoy, kar vpliva na občutljiva ekološka in astronomska območja. Zaradi močne povezave med svetlobnimi emisijami in družbenogospodarskimi kazalniki je poudarjena potreba po trajnostnih politikah na področju razsvetljave, s katerimi bi se zmanjšali negativni vplivi na okolje.

KLJUČNE BESEDE: svetlobno onesnaženje, daljinsko zaznavanje, geografski informacijski sistemi, prostorsko-časovna analiza, SNPP/VIIRS, urbanizacija, okoljska trajnost

The article was submitted for publication on June 11th, 2025.
Uredništvo je prejelo prispevek 11. junija 2025.

[1] Samsun Bahcesehir College Atakum Science and Technology High School, Samsun, Turkey
sarpdorukozturk2026@yahoo.com (https://orcid.org/0009-0006-6159-4852)

[2] Ondokuz Mayis University, Department of Geomatics Engineering, Samsun, Turkey
dzozturk@gmail.com (https://orcid.org/0000-0002-0684-3127)

1 Introduction

Light pollution refers to the harmful effects of excessive or misdirected artificial lighting, including skyglow, glare, light trespass, and over-illumination. These effects disrupt ecosystems, human health, astronomy, and energy efficiency (Chepesiuk 2009; Pan and Du 2021). Since the invention of electric lighting in the 19th century, global light emissions have steadily increased, particularly in urban areas, due to expanding residential, industrial, and commercial activity (Nurbandi et al. 2016; Levin and Zhang 2017; Cox et al. 2022). This increase has been further accelerated by uncontrolled urbanization (Hu et al. 2018; Gaston et al. 2023).

Excessive artificial nighttime lighting disrupts circadian rhythms, causes sleep disorders, and alters wildlife behavior, including feeding and migration patterns (Butt 2012; Hu et al. 2018; Brayley et al. 2022). It also impairs the visibility of celestial objects and reduces the effectiveness of astronomical instruments (Faid et al. 2024). Moreover, inefficient outdoor lighting wastes energy, leading to economic losses (Tong et al. 2022). Light pollution has thus become a growing concern across disciplines, including astronomy, environmental science, ecology, and public health (Chepesiuk 2009; Wu and Wang 2019; Green et al. 2022).

Light pollution is measured through both in situ methods and remote sensing (RS) (Mander et al. 2023). While tools like Sky Quality Meters (SQM) provide local precision, they lack large-scale coverage (Ji et al. 2024). RS enables wide-area monitoring of nocturnal lighting using satellite-based nighttime light (NTL) imagery, especially from the Defense Meteorological Satellite Program's Operational Linescan System (DMSP/OLS) and Suomi National Polar-orbiting Partnership's Visible Infrared Imaging Radiometer Suite (SNPP/VIIRS) satellites (Hu et al. 2018; Wu and Wang 2019). Compared to DMSP/OLS, SNPP/VIIRS provides higher spatial and radiometric resolution and filters out non-artificial light sources for greater accuracy (Levin and Zhang 2017; Ma et al. 2020).

However, several challenges remain in interpreting SNPP/VIIRS-derived trends. First, the satellite does not capture blue wavelengths characteristic of modern white Light Emitting Diode (LED) lighting. Second, the dataset is relatively limited, as SNPP/VIIRS only began recording nighttime radiance in late 2011, with data available for download from April 2012 onward (Carias et al. 2021; Levin 2025). Despite these constraints, SNPP/VIIRS remains a crucial dataset and is widely used to detect long-term urban brightness patterns and transient events such as wildfires or maritime activity (Cheon and Kim 2020; Yerli et al. 2021).

With the deployment of high spatial resolution NTL data from the Glimmer Imager for Urbanization (GIU) sensor aboard the Sustainable Development Goals Satellite 1 (SDGSAT-1) by the Chinese Academy of Sciences (CAS), new opportunities have emerged to address some of the current gaps in light pollution research (Xie et al. 2024). The GIU sensor provides multispectral NTL imagery with a 40-m resolution and panchromatic imagery at 10-m resolution. Importantly, these data are globally accessible since September 2022 (Yin et al. 2024), offering the highest quality NTL observations currently available and enabling the differentiation of light sources, including the effects of LED transitions, which are not always accurately captured by SNPP/VIIRS (Liu et al. 2024; Wang et al. 2024). Nevertheless, SNPP/VIIRS NTL data remain indispensable for long-term change detection compared to SDGSAT-1 (Xie et al. 2024). Importantly, recent studies indicate that NTL radiance values are highly variable, and that the effects of seasonal fluctuations and cultural events on NTL intensity must be carefully considered (Martinez et al. 2023; Dong et al. 2025). In change-detection studies, these effects can be minimized by using comparable time periods. Moreover, RS-derived NTL data are often validated using ground-based measurements (e.g., SQM) or high-resolution airborne imagery to improve accuracy and reliability (Guk and Levin 2020; Levin 2023).

Many studies have employed RS and geographic information systems (GIS) to analyze the spatial distribution and temporal dynamics of NTL intensity (Nurbandi et al. 2016; Levin and Zhang 2017; Yerli et al. 2021; Cox et al. 2022). However, most studies rely on conventional GIS techniques and focus on national or regional scales, with limited application of spatial statistical or algebraic methods. Consequently, localized patterns and urban-scale variations often remain underexplored.

Samsun, the most populous and economically developed city in Turkey's Black Sea region (Samsun Chamber of… 2022), encompasses ecologically critical zones such as the Kizilirmak Delta (a Ramsar site), the Yesilirmak Delta, and Lake Ladik (Eken et al. 2006), as well as one of Turkey's fifteen astronomical observatories, located in Atakum as listed by the Scientific and Technological Research Council of Turkey. Rapid urbanization, industrial expansion, and infrastructure development have led to significant losses in dark sky areas, affecting both urban and rural zones. Despite these challenges, academic research on light pollution

in Samsun remains scarce. Existing studies are limited to either a single district (Türk and Yavuz 2023) or national-scale data that ends in 2020 (Yerli et al. 2021), lacking detailed spatial analyses.

This study addresses these gaps by applying SNPP/VIIRS imagery to conduct a fine-grained, district-level analysis of Samsun from 2012 to 2024. By integrating RS and GIS with advanced spatial statistical and algebraic techniques, the study moves beyond descriptive mapping and establishes a quantitative framework to detect spatial heterogeneity and temporal trends in artificial lighting, which represents an approach that has rarely been applied in previous NTL studies.

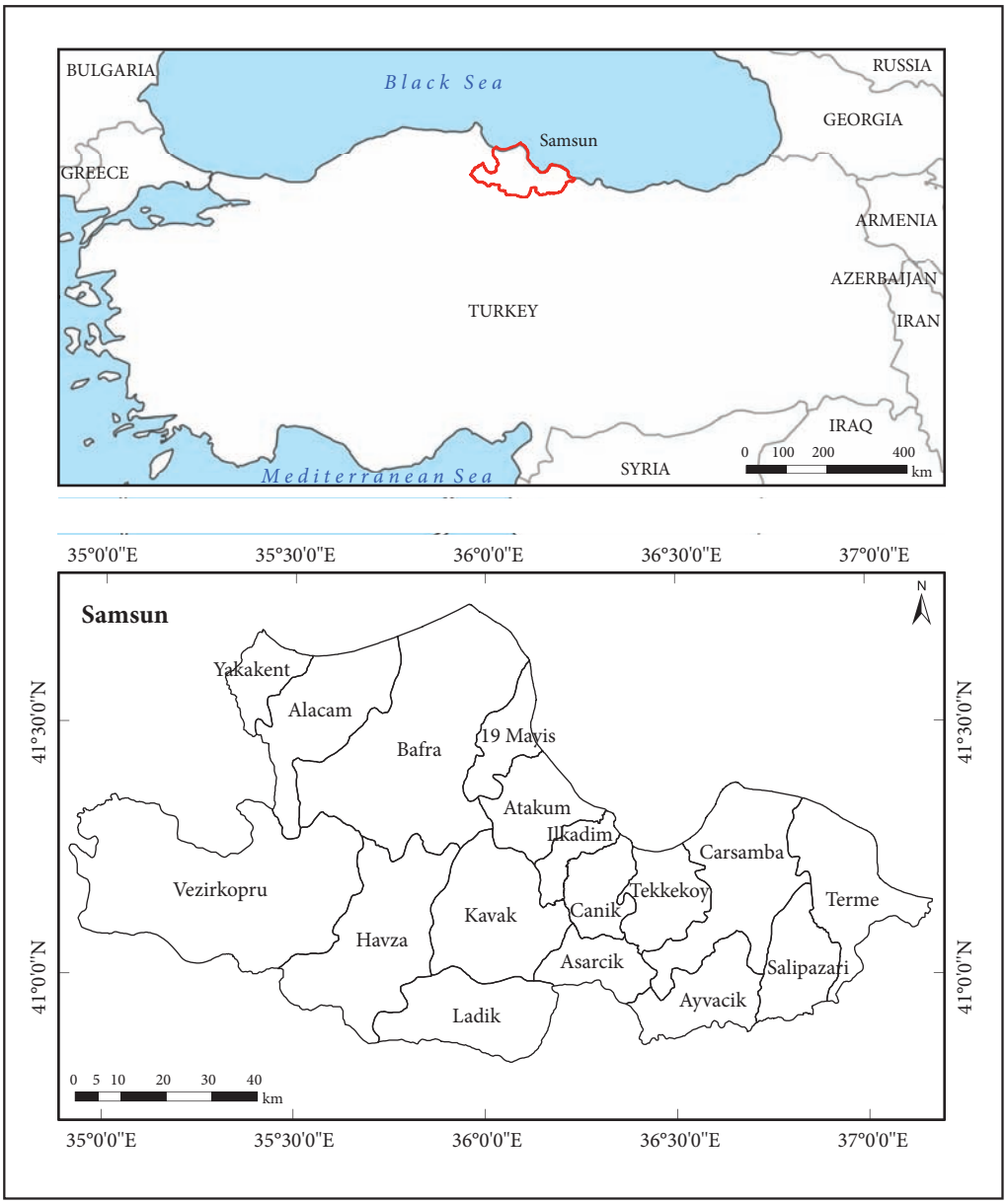

Figure 1: Study area: Samsun.

The study makes three primary contributions: (i) it demonstrates the effectiveness of RS and GIS integration in identifying light pollution patterns at the sub-city scale; (ii) it advances the underutilized application of spatial statistics and algebra in NTL research; and (iii) it provides a replicable methodology applicable to other rapidly urbanizing contexts. These methodological contributions are complemented by the study's regional focus, which provides a rare, spatially detailed assessment of a city with significant ecological and astronomical value. The findings provide practical insights for urban planning, sustainable environmental management, and dark sky conservation.

2 Study area

Samsun (Figure 1) is located in northern Turkey (40°50′–41°51′ N, 34°25′–37°08′ E), and by the data from General Directorate of Mapping, it covers approximately 9,730 km². According to data from Statistical Institute, Samsun had a population of around 1.4 million in 2024, making it the Black Sea region's most populous province (Öztürk and Gündüz 2019). Comprising 17 districts and a 210 km coastline, it serves as a metropolitan and industrial hub attracting internal migration (Samsun Chamber of … 2022).

Samsun is undergoing rapid urbanization, especially in coastal areas such as Atakum, Ilkadim, Canik, and Tekkekoy, which show the highest population growth (Ozturk 2017). According to the Socio-Economic Development Index (SEDI) by General Directorate of Development Agencies, Atakum ranks in the top tier and hosts both an astronomical observatory and a major tourism sector, while the other three districts fall into the second-highest tier.

While some districts experience intense urban growth, others contain ecologically sensitive zones vulnerable to light pollution. The Kizilirmak Delta (31,327 ha), located in 19 Mayis, Bafra, and Alacam, is one of Turkey's most biodiverse wetlands, home to 362 bird species and various habitats. It holds Ramsar, Natural Site, and Wildlife Development Area designations (General Directorate of … 2019). Similarly, the Yesilirmak Delta (20,658 ha) spans Carsamba, Tekkekoy, and Terme, supporting over 323 bird species and serving as a key habitat for waterfowl. Ladik Lake, a nationally important wetland, also hosts rich fish and bird biodiversity (Eken et al. 2006; General Directorate of … 2024).

3 Methodology

This study employs RS and GIS to assess district-level changes in light pollution in Samsun between 2012 and 2024. The primary data source is SNPP/VIIRS Day/Night Band (DNB) monthly cloud-free composite NTL imagery from 2012, 2015, 2018, 2021, and 2024. The values in SNPP/VIIRS DNB are expressed in nanowatts per square centimeter per steradian (nW/cm²/sr). Data processing was conducted in ArcGIS 10.3 (ESRI, Redlands, CA), using spatial statistics and algebra. With the Zonal Statistics tool, key metrics (minimum, maximum, mean, and standard deviation) were extracted for each district and Samsun overall. To visualize spatial variation, change maps (2012–2015, 2015–2018, 2018–2021, 2021–2024, and 2012–2024) were generated using Algebraic Change Mapping, and a range map (2012–2024) was produced with the Cell Statistics tool. Light emission values were classified into five categories to generate light pollution maps for each study year, and the area of each class was calculated to evaluate temporal trends. Finally, Pearson correlation analysis was performed using Multivariate Statistics tools to examine the relationship between mean light emission and variables such as population, population density, and SEDI scores. An overview of the methodological workflow is presented in Figure 2.

3.1 Data

This study utilizes SNPP/VIIRS DNB monthly cloud-free composite Version 1 imagery (Earth Observation Group, Colorado School of Mines 2025) to assess nighttime light emissions. SNPP/VIIRS DNB is a satellite-based dataset widely used in Earth system science for measuring visible and near-infrared nocturnal light (Wu and Wang 2019; Earth Data, NASA 2025). The cloud-free composite provides globally calibrated mosaics of monthly average observations, excluding stray light-affected data (Levin and Zhang 2017). The composites are produced by the Suomi National Polar Partnership, a NOAA (National Oceanic and

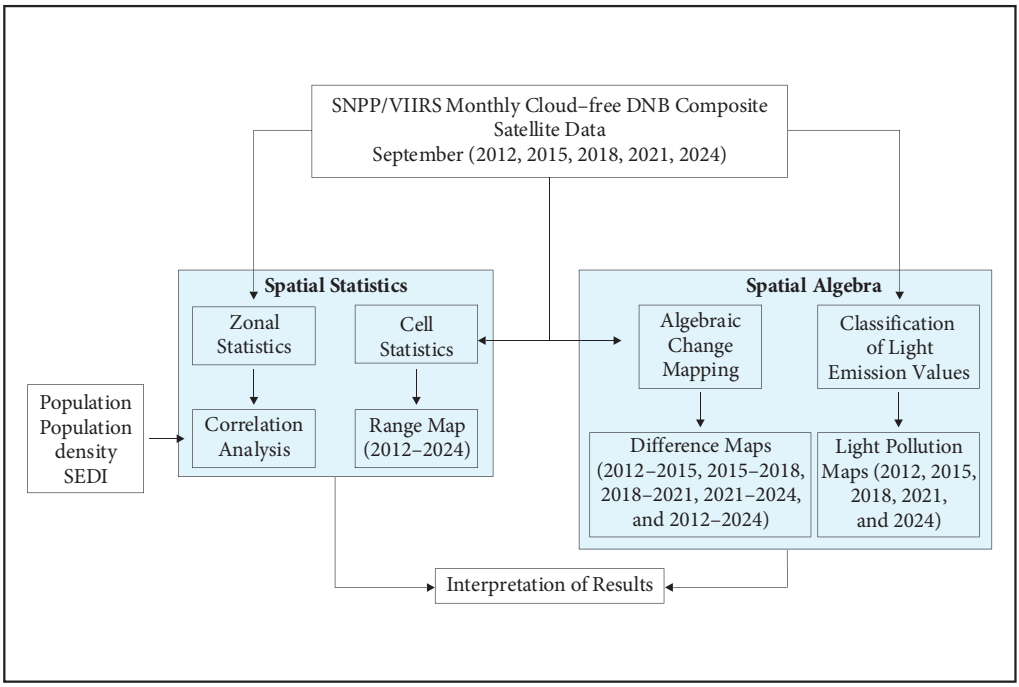

Figure 2: Workflow of the study.

Atmospheric Administration) and NASA (National Aeronautics and Space Administration) collaboration (Miller et al. 2013; Nurbandi et al. 2016). They are radiometrically calibrated and geometrically corrected, which ensures their suitability for direct scientific analysis (Levin 2017). This study used tile 2 (75N/060W) for the years 2012, 2015, 2018, 2021, and 2024, focusing on September due to its typically low cloud cover over Samsun. Data specifications of SNPP/VIIRS DNB are summarized in Table 1 according to the technical information published by NASA, Earth Data.

Additional data on population, population density, and SEDI were used to examine the relationship between light pollution and urban characteristics (Table 2). District-level population figures were sourced from the Statistical Institute, and density was calculated using population and district area data, with boundaries provided by the General Directorate of Mapping. SEDI scores and rankings, derived from 56 variables across six domains, were obtained from the data by General Directorate of Development Agencies. Central districts (Atakum, Ilkadim, Canik, Tekkekoy) show higher population, population density, and SEDI scores, whereas rural districts such as Ayvacik, Asarcik, Salipazari, Yakakent, and Vezirkopru have lower values, reflecting urban–rural contrasts.

Table 1: SNPP/VIIRS DNB data specifications.

Specification	Description
Image Resolution	15 arc seconds (~742 m at nadir)
Unit	nW/cm^2/sr
Coordinate Reference System	EPSG:4326 (Geographic Lat/Long)
Equatorial Crossing Time	1:30 PM (ascending)
Data Coverage	2012-01-02 to Present

Table 2: Area, population, population density, SEDI rank, and SEDI score of districts in Samsun (2012–2024).

District	Area (km^2)	SEDI rank	SEDI score	Population (Population density)				
				2012	2015	2018	2021	2024
19 Mayis	233.1	3	-0.137	24288 (104.2)	24627 (105.7)	26337 (113.0)	26366 (113.1)	28318 (121.5)
Alacam	598.2	4	-0.417	28315 (47.3)	26301 (44.0)	25854 (43.2)	24860 (41.6)	24686 (41.3)
Asarcik	254.5	5	-0.745	18215 (71.6)	17238 (67.7)	17628 (69.3)	16278 (64.0)	16128 (63.4)
Atakum	351.4	1	1.734	139730 (397.6)	169809 (483.2)	202618 (576.6)	238702 (679.3)	253437 (721.2)
Ayvacik	383.9	5	-0.784	22623 (58.9)	20619 (53.7)	21847 (56.9)	19436 (50.6)	19556 (50.9)
Bafra	1502.5	3	0.256	143366 (95.4)	141401 (94.1)	142210 (94.7)	142341 (94.7)	143600 (95.6)
Canik	262.2	2	0.553	92201 (351.6)	96541 (368.2)	97564 (372.1)	99369 (379.0)	100591 (383.6)
Carsamba	773.3	3	-0.015	136802 (176.9)	136775 (176.9)	138840 (179.5)	140439 (181.6)	141850 (183.4)
Havza	864.9	3	-0.124	43520 (50.3)	41146 (47.6)	40194 (46.5)	38872 (44.9)	38493 (44.5)
Ilkadim	154.8	2	1.343	312332 (2017.7)	321714 (2078.3)	332230 (2146.2)	340421 (2199.1)	325775 (2104.5)
Kavak	696.8	4	-0.331	20312 (29.2)	20130 (28.9)	21692 (31.1)	21260 (30.5)	25469 (36.6)
Ladik	543.2	4	-0.260	17274 (31.8)	16474 (30.3)	16734 (30.8)	16320 (30.0)	16309 (30.0)
Salipazari	349.0	5	-0.730	19379 (55.5)	18869 (54.1)	22923 (65.7)	19305 (55.3)	20046 (57.4)
Tekkekoy	326.5	2	0.650	48997 (150.1)	49843 (152.7)	52258 (160.1)	55369 (169.6)	58889 (180.4)
Terme	557.5	4	-0.202	73094 (131.1)	71910 (129.0)	72354 (129.8)	71366 (128.0)	71720 (128.6)
Vezirkopru	1672.2	5	-0.537	102212 (61.1)	97815 (58.5)	95569 (57.2)	91978 (55.0)	88564 (53.0)
Yakakent	204.5	5	-0.538	9062 (44.3)	8672 (42.4)	8864 (43.3)	8592 (42.0)	8945 (43.7)
Total (SAMSUN)	**9729.0**			**1227434 (126.2)**	**1255257 (129.0)**	**1309379 (134.6)**	**1344908 (138.2)**	**1354058 (139.2)**

3.2 Spatial statistical analysis

Spatial statistics involves applying statistical methods to geographically referenced data, where location is essential to analysis (Unwin 2009). These methods treat spatial attributes as variables, enabling detection of patterns and relationships (Forster 2000). This study employed three techniques: Zonal Statistics, Cell Statistics, and Multivariate Statistics.

Zonal statistics summarize raster data within defined zones such as administrative boundaries (Winsemius and Braaten 2023), helping to characterize regional patterns (Song et al. 2016). In this study, the Zonal Statistics as Table tool in ArcGIS was used to calculate the minimum, maximum, mean, and standard deviation of light emission values for each district. This enabled both temporal comparison and spatial trend analysis (Levin and Zhang 2017; Winsemius and Braaten 2023).

Cell statistics are local functions that generate new rasters by applying statistical operations (e.g., maximum, minimum, range) across multiple input rasters on a cell-by-cell basis (Ozturk and Kilic 2016). In this study, the Cell Statistics tool in ArcGIS was employed to determine the range of light emission values for each cell. This identified areas with the greatest temporal variation in light emissions (Li et al. 2008).

Multivariate statistics examine relationships among multiple variables or data layers. **Correlation analysis** is a commonly used multivariate statistical method that quantifies the strength and direction of linear relationships between variables (Ozturk and Kilic 2016). In this study, Pearson correlation analysis (Profillidis and Botzoris 2018; Xu 2020) was used to assess the linear relationship between mean light emission values and three urban variables: population, population density, and SEDI scores.

3.3 Spatial algebra

Spatial algebra is a mathematical framework comprising various algebraic, logical, and topological operations used to analyze spatial data (Kankanhalli et al. 1995; Li et al. 2002; Nobre et al. 2009). In this study, algebraic change mapping and the classification of light emission values were applied to analyze changes in light pollution.

Algebraic change detection uses image algebra to highlight temporal changes by calculating pixel-wise differences, producing a single-band image (Close et al. 2021). It is valued for simplicity, speed, and sensitivity to radiometric differences (Afify 2011; Goswami et al. 2022). This study used image differencing, subtracting values in an earlier image (Image 1) from a later one (Image 2), as shown in Equation 1 (Alphan 2011; Tenneson et al. 2023):

$$\text{Change} = \text{Image 2} - \text{Image 1} \quad \text{(Equation 1)},$$

To evaluate light pollution levels, SNPP/VIIRS **light emission values are categorized** based on ecological and astronomical thresholds. The International Astronomical Union recommends a maximum artificial sky brightness of no more than 10% above natural levels (~0.25 mcd/m²) for observatory locations (Lowenthal et al. 2022). In ecological contexts, artificial light exceeding certain thresholds can disrupt wildlife and ecosystems (Widmer et al. 2022).

Building on the classification by Hügli (2021), which refines earlier schemes by Hale et al. (2018) and Hale and Arlettaz (2019), light emission values are divided into five categories (Table 3). In this classification, a threshold of 2 nW/cm²/sr represents the typical radiance level associated with small villages or sparsely populated residential areas. Radiance values around 10 nW/cm²/sr are characteristic of larger towns with relatively high population densities. In extensive urban settlements, where various lighting systems are employed, measured values commonly reach approximately 20 nW/cm²/sr (Widmer et al. 2022). Light emissions exceeding 2 nW/cm²/sr are expected to have at least a minor impact on ecosystems and wildlife (Hale et al. 2018; Widmer et al. 2022). In this study, light emission values were classified according to the Table 3.

Table 3: Classification of light emission values.

Radiance (nW/cm²/sr)	Category
< 0.5	Lowest light emission
0.5–2	Very low light emission
2–10	Low light emission
10–20	Medium light emission
>=20	High light emission

4 Results

This section presents the findings from the analysis of SNPP/VIIRS data across Samsun's districts from 2012 to 2024. The results reveal spatial and temporal variations in light intensity, reflecting trends in urbanization, industrial activity, and infrastructure development. The analysis is organized into four components:

(i) zonal statistics summarizing district-level light emissions; (ii) difference and range mapping highlighting temporal variation; (iii) light pollution classification showing the spatial distribution of artificial lighting; and (iv) correlation analysis exploring links between light intensity and socio-economic variables.

4.1 Zonal statistics

Zonal statistics were computed using SNPP/VIIRS data for 2012, 2015, 2018, 2021, and 2024. Key metrics per district are summarized in Table 4, and temporal trends in mean light intensity are shown in Figure 3.

Table 4: Summary statistics of SNPP/VIIRS light intensity (nW/cm^2/sr) by district (2012–2024).

	2012		2015		2018		2021		2024	
District	min **mean**	max **std dev**	min **mean**	max **std dev**	min **mean**	max **std dev**	min **mean**	max **std dev**	min **mean**	max **std dev**
19 Mayis	0.15 **1.61**	27.32 **2.99**	0.09 **1.71**	23.77 **2.82**	0.24 **2.34**	33.74 **3.62**	0.32 **2.92**	34.51 **3.88**	0.47 **3.32**	42.55 **3.93**
Alacam	0.08 **0.50**	19.80 **1.14**	0.00 **0.69**	51.25 **2.49**	0.11 **1.03**	46.95 **2.67**	0.20 **1.34**	57.11 **3.07**	0.27 **1.38**	46.84 **2.72**
Asarcik	0.14 **0.40**	12.36 **0.61**	0.03 **0.44**	12.45 **0.81**	0.14 **0.69**	17.63 **1.11**	0.28 **0.96**	22.11 **1.31**	0.40 **1.18**	18.93 **1.30**
Atakum	0.15 **4.29**	88.36 **11.37**	0.10 **4.90**	70.07 **10.85**	0.21 **5.62**	79.30 **12.32**	0.34 **5.73**	75.19 **12.24**	0.44 **6.01**	67.93 **11.71**
Ayvacik	0.12 **0.43**	9.08 **0.63**	0.00 **0.39**	10.94 **0.76**	0.09 **0.58**	13.23 **0.80**	0.22 **0.99**	18.38 **1.12**	0.33 **1.29**	14.32 **1.07**
Bafra	0.07 **0.65**	51.43 **2.28**	0.00 **0.72**	57.49 **2.91**	0.11 **1.08**	72.36 **3.64**	0.16 **1.51**	83.91 **4.07**	0.26 **1.71**	67.22 **3.69**
Canik	0.17 **1.77**	65.28 **6.07**	0.06 **2.32**	77.17 **7.88**	0.25 **2.79**	69.99 **8.54**	0.42 **2.86**	80.91 **7.92**	0.55 **3.07**	60.84 **6.68**
Carsamba	0.14 **1.25**	45.15 **2.83**	0.00 **1.53**	42.16 **3.50**	0.10 **1.90**	47.18 **3.91**	0.29 **2.76**	65.60 **4.87**	0.38 **3.27**	60.16 **4.43**
Havza	0.09 **0.60**	57.33 **2.25**	0.00 **0.64**	71.98 **2.80**	0.10 **0.99**	61.37 **3.05**	**0.25** **1.18**	54.52 **2.79**	0.34 **1.38**	53.61 **2.94**
Ilkadim	0.23 **9.43**	121.14 **18.79**	0.26 **10.14**	88.66 **17.08**	0.46 **12.09**	89.48 **19.58**	0.59 **11.51**	85.76 **17.94**	0.89 **10.64**	73.66 **15.09**
Kavak	0.13 **0.64**	33.68 **1.95**	0.02 **0.95**	43.63 **2.85**	0.16 **1.09**	40.88 **2.81**	0.25 **1.21**	39.71 **2.71**	0.36 **1.42**	48.09 **2.70**
Ladik	0.10 **0.49**	40.94 **1.62**	0.00 **0.52**	45.22 **1.97**	0.14 **0.80**	51.94 **2.33**	0.25 **0.97**	0.25 **2.19**	0.30 **1.19**	47.14 **2.37**
Salipazari	0.14 **0.50**	17.10 **0.75**	0.03 **0.47**	13.84 **0.70**	0.18 **0.79**	26.09 **1.30**	0.29 **1.11**	18.69 **1.24**	0.48 **1.45**	17.52 **1.25**
Tekkekoy	0.17 **2.35**	42.84 **5.49**	0.00 **3.20**	171.04 **9.61**	0.21 **3.95**	75.96 **9.32**	0.38 **4.38**	146.97 **9.70**	0.53 **4.41**	48.79 **7.18**
Terme	0.15 **1.15**	50.92 **2.58**	0.04 **1.40**	48.43 **1.40**	0.22 **1.94**	59.86 **3.70**	0.32 **2.58**	49.14 **3.66**	0.47 **2.95**	53.98 **3.57**
Vezirkopru	0.09 **0.41**	39.83 **1.66**	0.00 **0.35**	51.16 **1.90**	0.10 **0.62**	71.63 **2.63**	0.15 **0.86**	73.40 **2.94**	0.28 **1.02**	70.15 **2.84**
Yakakent	0.10 **0.35**	9.54 **0.73**	0.00 **0.33**	10.86 **0.86**	0.10 **0.92**	29.78 **2.91**	0.25 **1.05**	32.89 **2.75**	0.31 **1.06**	23.64 **2.16**
SAMSUN	0.07 **1.02**	121.14 **4.22**	0.00 **1.18**	171.04 **4.66**	0.09 **1.57**	89.48 **5.26**	0.15 **1.90**	146.97 **5.28**	0.26 **2.10**	73.66 **4.76**

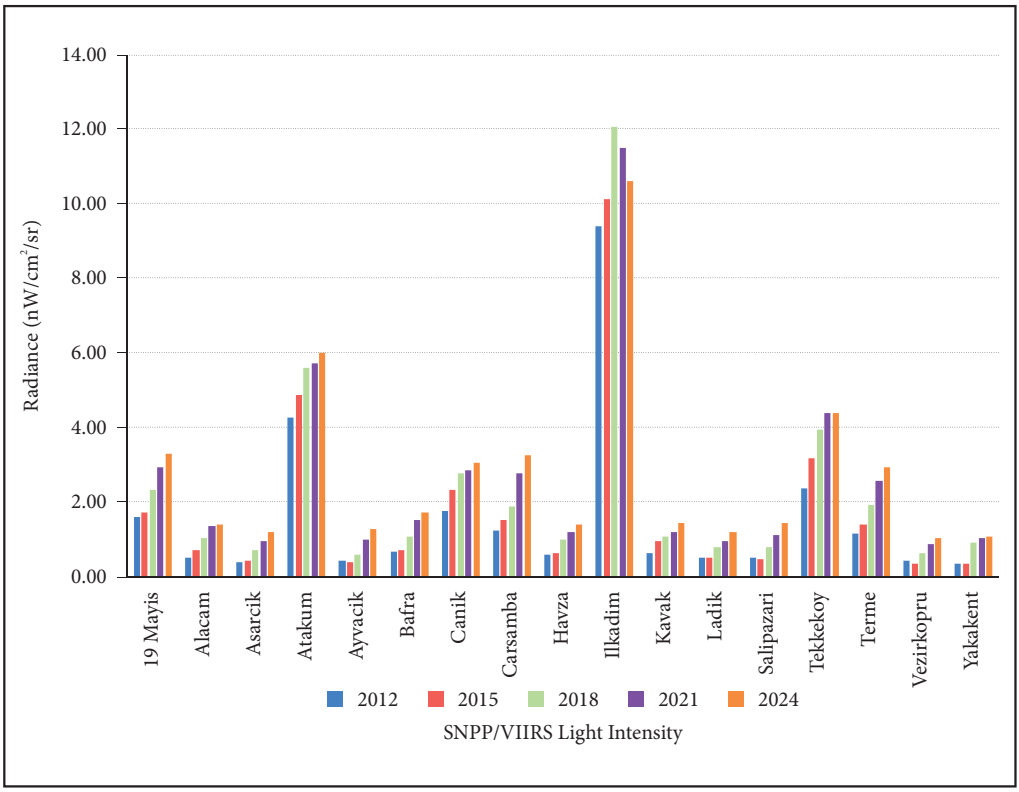

Figure 3: Change in mean SNPP/VIIRS light intensity.

The results show a general upward trend in light intensity across most districts between 2012 and 2024. Among all districts, Atakum and Ilkadim consistently recorded the highest mean light levels throughout the study period. While a sharp increase occurred from 2012 to 2018, the growth rate slowed in 2021 and 2024. Notably, Ilkadim reached a peak mean intensity of 12.09 nW/cm²/sr in 2018, representing the highest value across all districts and years. Following 2018, radiance levels in Ilkadim experienced a decline, which is directly attributable to the implementation of municipal energy conservation and lighting policies under the framework of Samsun Metropolitan Municipality's sustainable energy strategies (Samsun Metropolitan … 2019).

Canik and Tekkekoy showed a steady increase, peaking in 2024. Similarly, districts with prominent industrial and commercial zones, such as Bafra, Carsamba, Terme, Havza, and Kavak, experienced a consistent increase in light intensity over the years. Conversely, more rural and low-population districts (e.g., 19 Mayis, Alacam, Asarcik, Yakakent, Vezirkopru, Salipazari, and Ladik) exhibited consistently low values, with a gradual increase over time. Overall, the upward trends observed in most districts up to 2018 appear to have partially decelerated in the period following 2018.

4.2 Difference and range maps

Difference and range maps were generated using SNPP/VIIRS data (2012–2024) to analyze spatial and temporal variations in light emissions (Figure 4). Image differencing was applied to consecutive intervals and the full study period, with positive values indicating increases and negative values representing decreases. The range map, calculated as the per-pixel difference between maximum and minimum values across

all years, highlights maximum variation at each location. In Figure 4, colors are scaled to each period's min–max values, highlighting relative differences between districts.

Temporal trends in light emissions indicate distinct phases of urban expansion. Between 2012 and 2015, significant light emission increases were observed in the coastal districts of Atakum, Ilkadim, Canik, and Tekkekoy, particularly along Atakum's coastal strip and the Canik-Tekkekoy corridor. These increases align with rapid urban development and expanding infrastructure. From 2015 to 2018, light pollution continued to grow in these central districts but also began to spread inland, suggesting the emergence of new residential and commercial zones. In 2018–2021, the spatial spread of light pollution accelerated, extending from core urban areas to peripheral and interior districts, indicating a broader geographical expansion of artificial lighting. By 2021–2024, nearly all districts experienced increased emissions, highlighting intensified urban sprawl and the proliferation of artificial light even in rural areas. The observed decline in certain areas after 2018 is attributable to energy efficiency measures and urban lighting policies implemented under the framework of Samsun Metropolitan Municipality's sustainable energy strategies (Samsun Metropolitan … 2019). Upgrading streetlights to LED technology, implementing dimming, and optimizing lighting schedules directly led to reduced light emissions, reflecting the municipality's efforts to balance illumination needs with environmental considerations. Furthermore, this slowdown was reinforced by reduced economic activity following the COVID-19 pandemic.

The long-term difference map (2012–2024) confirms a net increase in light emissions across Samsun, with hotspots in urban coastal corridors and industrial transport zones, while the range map (2012–2024) reveals the highest variability in central and coastal districts, while rural areas display minimal change, reflecting relatively stable light conditions over time. Comparing the difference (2012–2024) and range (2012–2024) maps reveals similar spatial patterns, indicating that light emission trends have generally followed a stable, unidirectional trajectory with minimal fluctuations. Central and coastal areas have undergone the most dramatic changes, driven by concentrated urbanization, while rural districts remain less affected by artificial lighting expansion.

4.3 Light pollution classification

Figure 5 displays classified light pollution maps for 2012, 2015, 2018, 2021, and 2024 based on SNPP/VIIRS satellite data and categorized using the thresholds defined in Table 3. These maps visualize the spatial distribution of light emissions and their progression over time, revealing a clear and steady increase in artificial lighting, particularly in urban and peri-urban areas.

Table 5: Area (km^2) and percentage distribution of light emission classes in Samsun (2012–2024).

Year	Lowest	Very low	Low	Medium	High	Total area
2012	6791.8 (69.8%)	2412.0 (24.8%)	351.4 (3.6%)	87.6 (0.9%)	85.9 (0.9%)	9729
2015	6368.8 (65.5%)	2644.8 (27.2%)	493.9 (5.1%)	110.9 (1.1%)	110.3 (1.1%)	9729
2018	4935.1 (50.7%)	3804.6 (39.1%)	724.9 (7.5%)	129.1 (1.3%)	135.0 (1.4%)	9729
2021	3309.3 (34.0%)	4776.7 (49.1%)	1362.5 (14.0%)	136.7 (1.4%)	143.6 (1.5%)	9729
2024	1853.5 (19.1%)	5584.6 (57.4%)	2005.6 (20.6%)	145.5 (1.5%)	139.5 (1.4%)	9729

Figure 4: Difference and range maps of light emissions (2012–2024). ► p. 76–77
Figure 5: Classified light pollution maps (2012, 2015, 2018, 2021, and 2024). ► p. 78–79

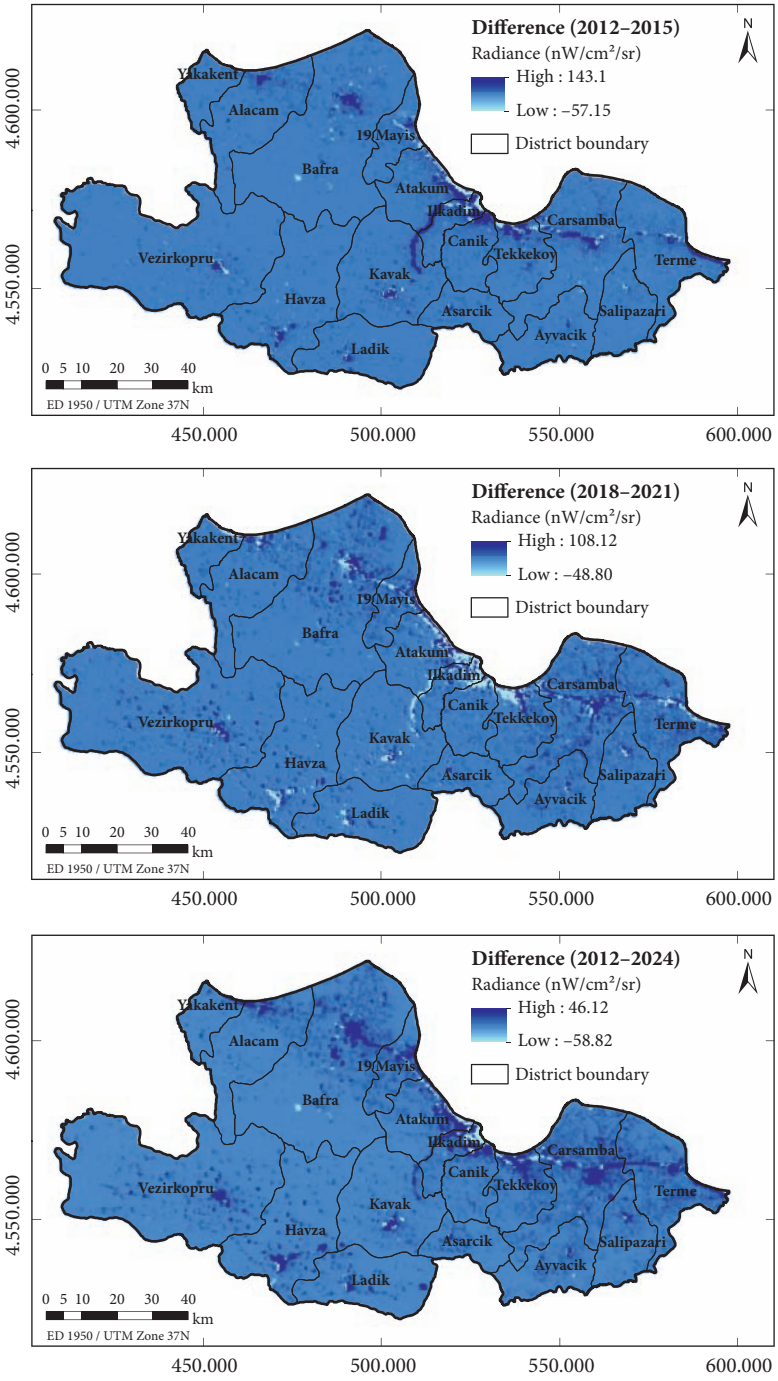
Difference (2012–2015)
Radiance (nW/cm²/sr)
High : 143.1
Low : –57.15
District boundary
N
Yakakent
Alacam
19 Mayis
Bafra
Atakum
Ilkadim
Carsamba
Canik
Tekkekoy
Terme
Vezirkopru
Kavak
Havza
Asarcik
Salipazari
Ayvacik
Ladik
0 5 10 20 30 40
km
ED 1950 / UTM Zone 37N
4.600.000
4.550.000
450.000
500.000
550.000
600.000
Difference (2018–2021)
Radiance (nW/cm²/sr)
High : 108.12
Low : –48.80
District boundary
N
Yakakent
Alacam
19 Mayis
Bafra
Atakum
Ilkadim
Carsamba
Canik
Tekkekoy
Terme
Vezirkopru
Kavak
Havza
Asarcik
Salipazari
Ayvacik
Ladik
0 5 10 20 30 40
km
ED 1950 / UTM Zone 37N
4.600.000
4.550.000
450.000
500.000
550.000
600.000
Difference (2012–2024)
Radiance (nW/cm²/sr)
High : 46.12
Low : –58.82
District boundary
N
Yakakent
Alacam
19 Mayis
Bafra
Atakum
Ilkadim
Carsamba
Canik
Tekkekoy
Terme
Vezirkopru
Kavak
Havza
Asarcik
Salipazari
Ayvacik
Ladik
0 5 10 20 30 40
km
ED 1950 / UTM Zone 37N
4.600.000
4.550.000
450.000
500.000
550.000
600.000

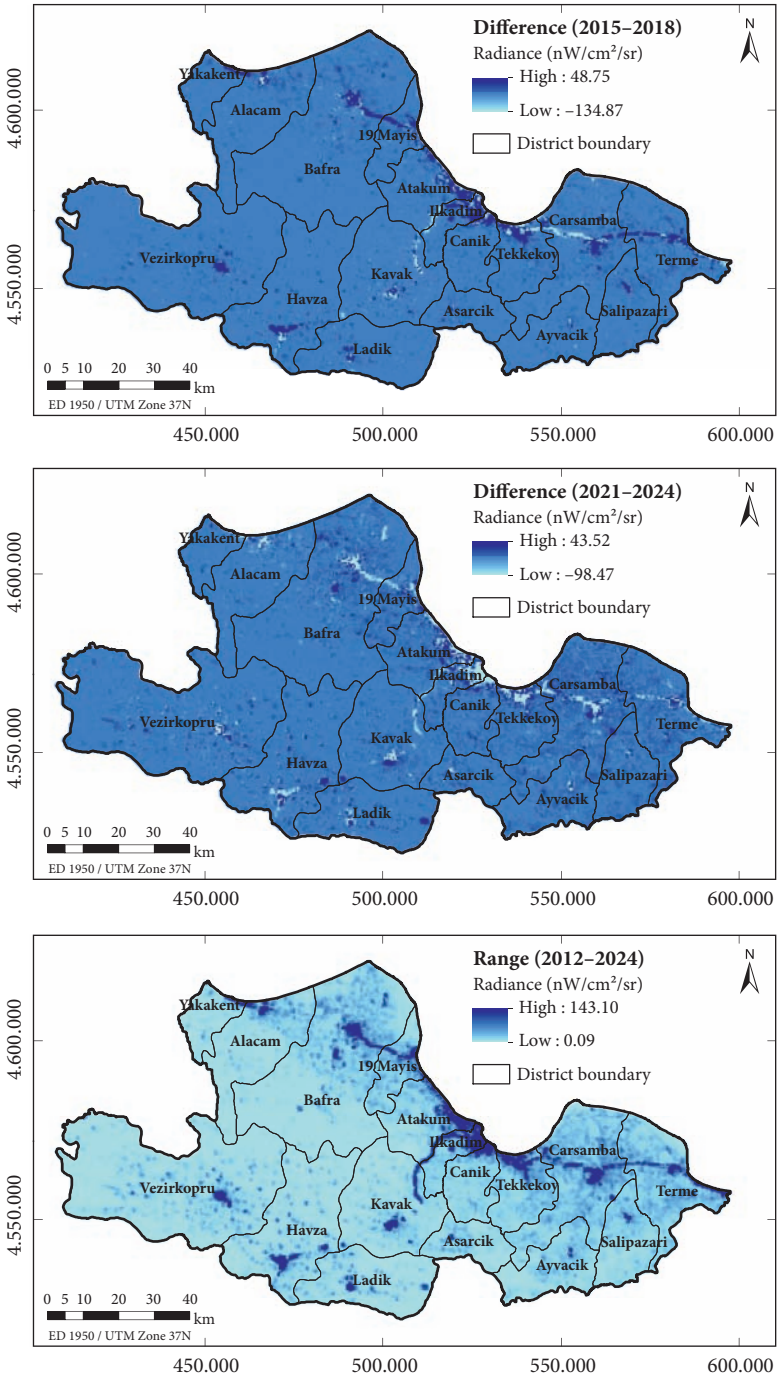

Content by: Sarp Doruk Ozturk
Map by: Sarp Doruk Ozturk, Derya Ozturk
Source: SNPP/VIIRS, Earth Observation Group

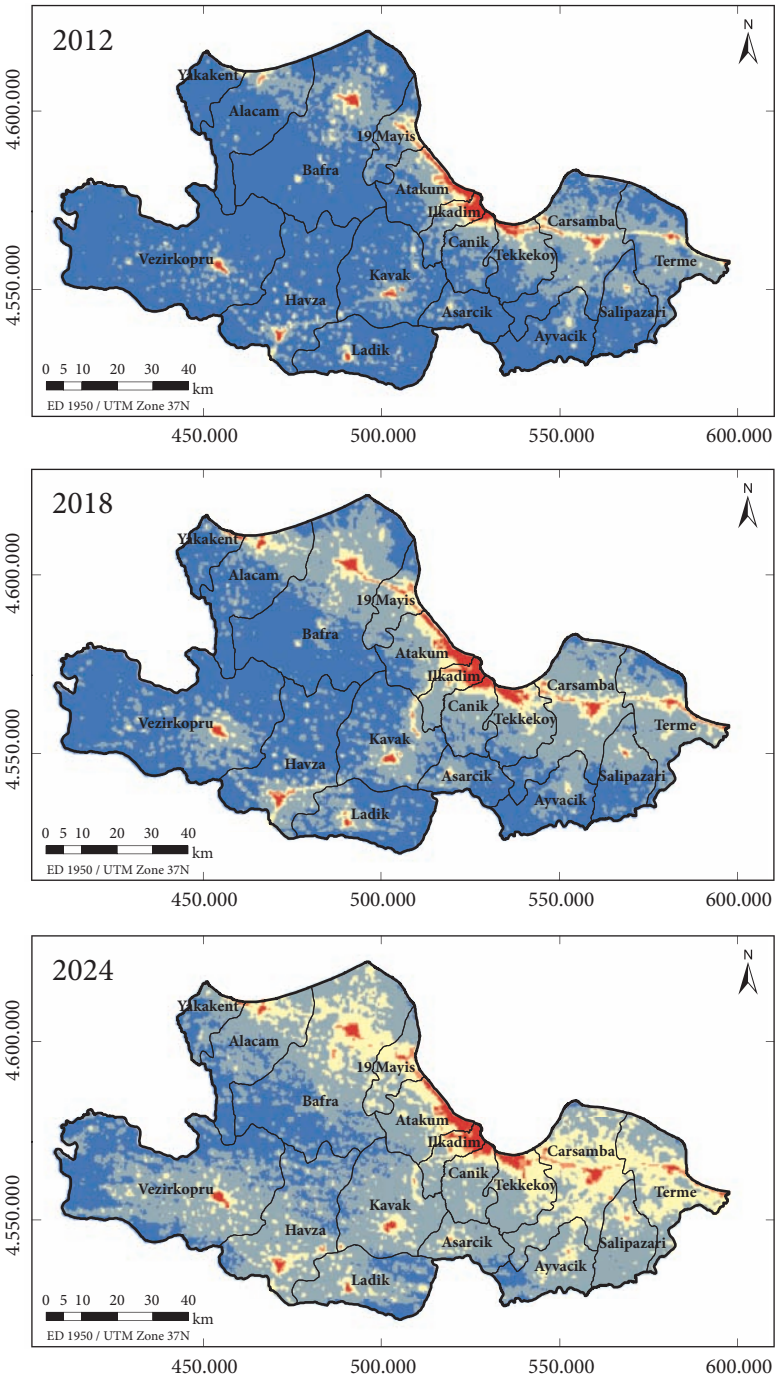
2012
2018
2024
N
Yakakent
Alacam
19 Mayis
Bafra
Atakum
Ilkadim
Carsamba
Canik
Tekkekoy
Terme
Vezirkopru
Kavak
Havza
Asarcik
Salipazari
Ayvacik
Ladik
0 5 10 20 30 40
km
ED 1950 / UTM Zone 37N
4.600.000
4.550.000
450.000
500.000
550.000
600.000

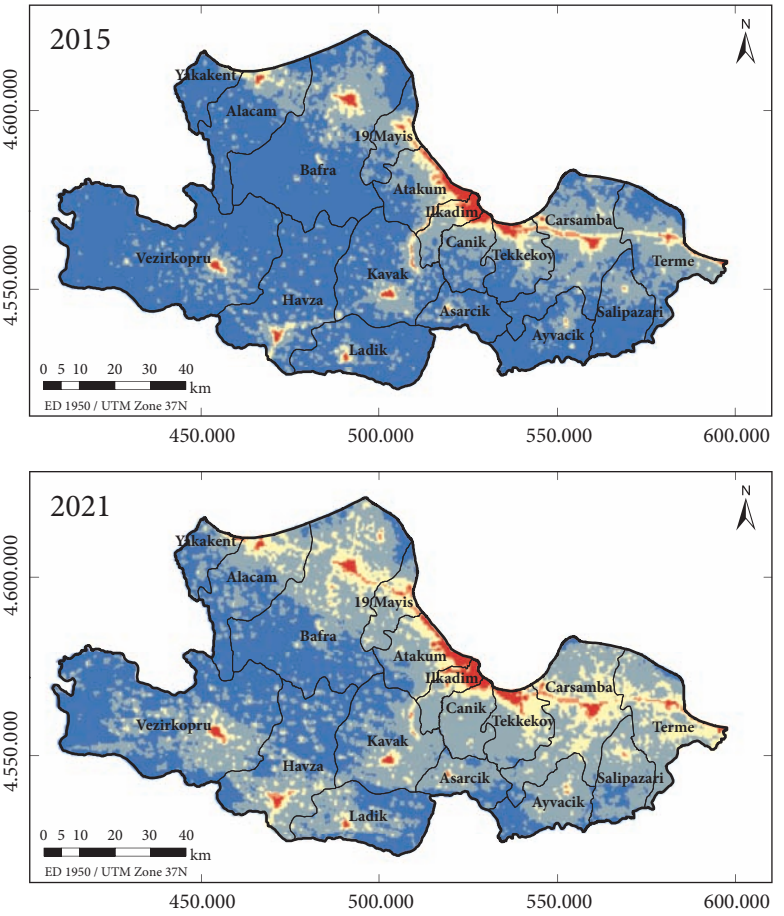

Radiance (nW/cm²/sr)	**Classification**
< 0.5	Lowest light emission
0.5–2	Very low light emission
2–10	Low light emission
10–20	Medium light emission
> 20	High light emission
District boundary	

Conte nt by: Sarp Doruk Ozturk
Map by: Sarp Doruk Ozturk, Derya Ozturk
Source : SNPP/VIIRS, Earth Observation Group

In 2012, the highest light intensities were concentrated in the central districts of Atakum, Ilkadim, Canik, and Tekkekoy, forming a bright corridor along the Middle Black Sea coastal road. In contrast, rural and inland regions showed predominantly low emission levels. By 2015, emissions intensified in central districts and along key transportation routes, indicating early signs of urban expansion and infrastructure growth. The year 2018 marked a notable shift, with increased emissions spreading inland from the coast. Significant growth was observed in new residential zones, commercial centers, and industrial areas, especially in Atakum, Ilkadim, and eastern Tekkekoy. Between 2018 and 2021, light pollution expanded further into peripheral districts, reflecting continued urbanization and rising infrastructure development. By 2024,

Table 6: Area (km^2) and percentage distribution of light emission classes by district (2012 and 2024).

District	Year	Lowest	Very low	Low	Medium	High	Total
19 Mayis	2012	89.2 (38.3%)	107.6 (46.1%)	27.0 (11.6%)	8.7 (3.7%)	0.6 (0.3%)	233.1
19 Mayis	2024	2.6 (1.1%)	112.7 (48.3%)	102.2 (43.9%)	13.7 (5.9%)	1.9 (0.8%)	233.1
Alacam	2012	464.0 (77.6%)	118.8 (19.9%)	13.0 (2.2%)	2.4 (0.4%)	0.0 (0.0%)	598.2
Alacam	2024	160.9 (26.9%)	347.4 (58.1%)	81.3 (13.6%)	5.6 (0.9%)	2.9 (0.5%)	598.2
Asarcik	2012	217.5 (85.5%)	33.8 (13.3%)	3.1 (1.2%)	0.2 (0.1%)	0.0 (0.0%)	254.5
Asarcik	2024	20.7 (8.1%)	205.3 (80.7%)	27.2 (10.7%)	1.3 (0.5%)	0.0 (0.0%)	254.5
Atakum	2012	137.0 (39.0%)	137.6 (39.2%)	37.6 (10.7%)	17.7 (5.0%)	21.5 (6.1%)	351.4
Atakum	2024	8.0 (2.3%)	191.5 (54.5%)	101.9 (29.0%)	15.8 (4.5%)	34.2 (9.7%)	351.4
Ayvacik	2012	313.3 (81.6%)	63.8 (16.6%)	6.8 (1.8%)	0.0 (0.0%)	0.0 (0.0%)	383.9
Ayvacik	2024	54.2 (14.1%)	269.8 (70.3%)	58.8 (15.3%)	1.1 (0.3%)	0.0 (0.0%)	383.9
Bafra	2012	1141.9 (76.0%)	308.0 (20.5%)	41.3 (2.7%)	4.5 (0.3%)	6.8 (0.4%)	1502.5
Bafra	2024	426.5 (28.4%)	738.7 (49.2%)	316.1 (21.0%)	11.6 (0.8%)	9.6 (0.6%)	1502.5
Canik	2012	121.5 (46.4%)	115.8 (44.1%)	14.5 (5.5%)	4.3 (1.7%)	6.1 (2.3%)	262.2
Canik	2024	0.0 (0.0%)	192.6 (73.5%)	54.8 (20.9%)	5.9 (2.3%)	8.8 (3.4%)	262.2
Carsamba	2012	288.1 (37.3%)	417.8 (54.0%)	51.9 (6.7%)	11.7 (1.5%)	3.7 (0.5%)	773.3
Carsamba	2024	9.8 (1.3%)	324.8 (42.0%)	404.5 (52.3%)	23.8 (3.1%)	10.4 (1.4%)	773.3
Havza	2012	709.5 (82.0%)	125.7 (14.5%)	24.3 (2.8%)	2.6 (0.3%)	2.9 (0.3%)	864.9
Havza	2024	181.7 (21.0%)	566.4 (65.5%)	104.7 (12.1%)	8.0 (0.9%)	4.2 (0.5%)	864.9
Ilkadim	2012	36.7 (23.7%)	61.6 (39.8%)	22.3 (14.4%)	10.3 (6.6%)	24.0 (15.5%)	154.8
Ilkadim	2024	0.0 (0.0%)	65.0 (42.0%)	45.8 (29.6%)	13.7 (8.8%)	30.4 (19.6%)	154.8
Kavak	2012	536.6 (77.0%)	140.4 (20.1%)	13.2 (1.9%)	3.9 (0.6%)	2.7 (0.4%)	696.8
Kavak	2024	73.1 (10.5%)	534.9 (76.8%)	79.7 (11.4%)	4.8 (0.7%)	4.2 (0.6%)	696.8
Ladik	2012	460.9 (84.8%)	70.1 (12.9%)	10.0 (1.8%)	0.8 (0.1%)	1.4 (0.3%)	543.2
Ladik	2024	136.5 (25.1%)	349.0 (64.2%)	54.0 (9.9%)	1.9 (0.4%)	1.8 (0.3%)	543.2
Salipazari	2012	257.7 (73.8%)	86.8 (24.9%)	3.9 (1.1%)	0.6 (0.2%)	0.0 (0.0%)	349.0
Salipazari	2024	0.8 (0.2%)	293.7 (84.2%)	52.7 (15.1%)	1.8 (0.5%)	0.0 (0.0%)	349.0
Tekkekoy	2012	125.7 (38.5%)	151.0 (46.2%)	27.8 (8.5%)	11.4 (3.5%)	10.6 (3.2%)	326.5
Tekkekoy	2024	0.0 (0.0%)	165.8 (50.8%)	128.5 (39.3%)	14.8 (4.5%)	17.5 (5.4%)	326.5
Terme	2012	190.3 (34.1%)	323.5 (58.0%)	37.3 (6.7%)	4.3 (0.8%)	2.1 (0.4%)	557.5
Terme	2024	2.3 (0.4%)	249.7 (44.8%)	284.9 (51.1%)	15.9 (2.9%)	4.8 (0.9%)	557.5
Vezirkopru	2012	1512.7 (90.5%)	138.7 (8.3%)	13.2 (0.8%)	4.2 (0.2%)	3.4 (0.2%)	1672.2
Vezirkopru	2024	702.2 (42.0%)	860.6 (51.5%)	97.6 (5.8%)	4.2 (0.2%)	7.6 (0.5%)	1672.2
Yakakent	2012	189.1 (92.5%)	11.1 (5.4%)	4.3 (2.1%)	0.0 (0.0%)	0.0 (0.0%)	204.5
Yakakent	2024	74.1 (36.2%)	116.9 (57.2%)	10.8 (5.3%)	1.6 (0.8%)	1.1 (0.6%)	204.5

artificial lighting had reached its highest levels across all years, with a noticeable spread of medium and high-emission areas in core districts and an expanding footprint of low-emission lighting in previously unlit rural zones.

Table 5 quantifies the area and percentage distribution of each light emission class across Samsun from 2012 to 2024. The most significant change is the sharp decline in »Lowest« light emission areas, from 69.8% (6791.8 km²) in 2012 to just 19.1% (1853.5 km²) in 2024, representing a reduction of over 50 percentage points. This decline is mirrored by an increase in »Very low« and »Low« categories, indicating that previously dark areas are now exposed to artificial light. Although the »Medium« and »High« categories have not expanded as dramatically, their steady growth reflects an increased concentration of artificial lighting, particularly in commercial and industrial zones.

Table 6 presents the spatial breakdown of light emission classes by district for 2012 and 2024. The »Lowest« emission class declined significantly across all districts and was entirely eliminated in Canik, Ilkadim, and Tekkekoy, underscoring intensified urbanization and infrastructure development. The expansion of »Very low« and »Low« classes across most districts reflects widespread electrification, rural development, and urban sprawl. While increases in »Medium« and »High« categories were more modest in terms of area, their concentration in urban cores and industrial zones points to localized intensification of artificial lighting. Notably, even traditionally rural districts such as Bafra, Carsamba, Terme, and 19 Mayis began transitioning into higher light emission classes, likely due to increased coastal development and transportation activity.

To further illustrate the transformation of previously dark areas and the potential ecological impact of artificial lighting, Figure 6 shows a map of regions with radiance lower than 2 nW/cm²/sr as well as areas where light emissions exceed this threshold for the years 2012, 2015, 2018, 2021, and 2024. This map illustrates the progressive reduction of »dark areas« over time, while regions where light emissions exceed 2 nW/cm²/sr, a level associated with measurable impacts on ecosystems and wildlife (Hale et al. 2018; Widmer et al. 2022), have expanded, reflecting the increasing spread of ecologically critical artificial lighting.

4.4 Correlation analysis

To explore the drivers of light emissions, a correlation analysis was conducted between mean SNPP/VIIRS light emission values and three variables: population, population density, and SEDI score. Across all years, correlations with population remained consistently strong ($r \geq 0.85$), while correlations with population density were higher ($r \geq 0.94$), highlighting the predominant influence of population concentration on light intensity and, by extension, urbanization. Correlations with SEDI were also substantial ($r \geq 0.80$), indicating that areas with greater artificial lighting correspond to more socio-economically developed regions characterized by denser infrastructure, services, and economic activity. Yearly correlation coefficients for all variables are summarized in Table 7.

Table 7: Correlation coefficients of mean light emission with population, population density, and SEDI score.

Relationship	2012	2015	2018	2021	2024
r (Mean light emission-Population)	0.85	0.86	0.86	0.87	0.87
r (Mean light emission-Population density)	0.96	0.95	0.96	0.95	0.94
r (Mean light emission-SEDI score)	0.80	0.82	0.81	0.82	0.84

Note: All correlation coefficients are statistically significant at $p < 0.001$.

Figure 6: Spatial distribution of areas exceeding the ecological threshold of 2 nW/cm²/sr in Samsun for 2012, 2015, 2018, 2021, and 2024. ➤ p. 82–83

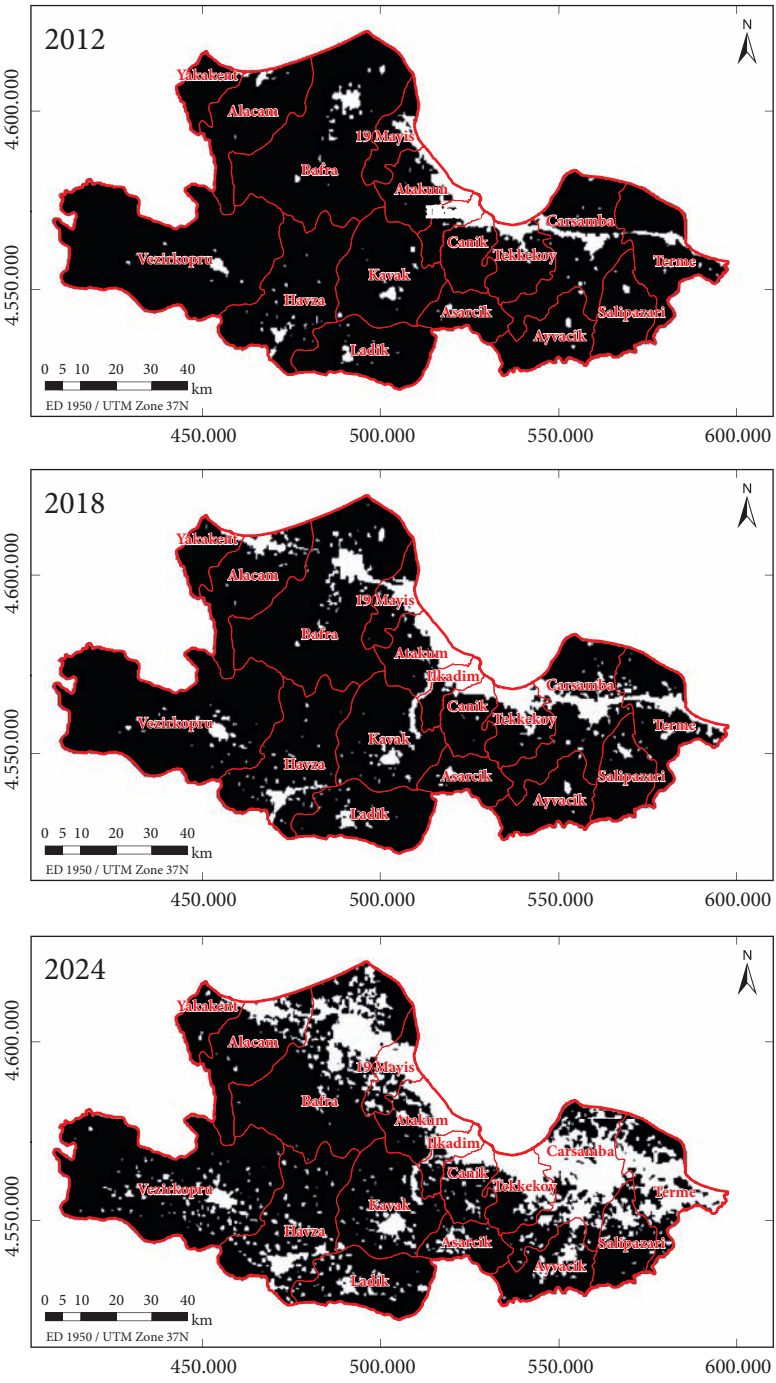
2012
2018
2024
N
Yakakent
Alacam
19 Mayis
Bafra
Atakum
Ilkadim
Carsamba
Canik
Tekkekoy
Terme
Vezirkopru
Kavak
Havza
Asarcik
Salipazari
Ayvacik
Ladik
0 5 10 20 30 40
km
ED 1950 / UTM Zone 37N
4.600.000
4.550.000
450.000
500.000
550.000
600.000

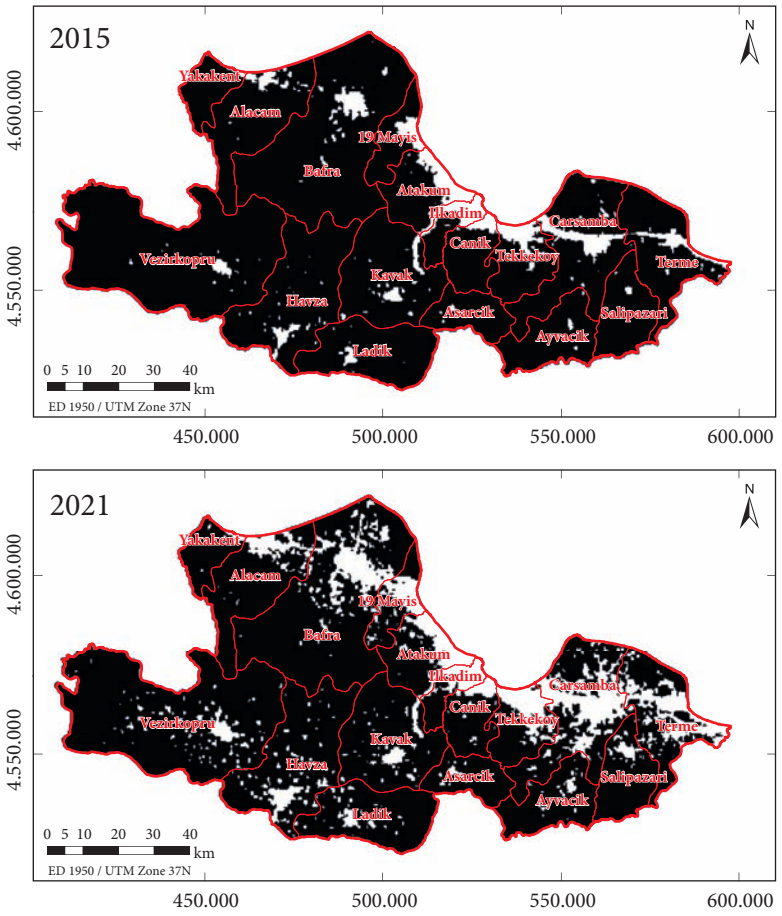

Areas Exceeding Critical Light Emission Thresh old (> 2 nW/cm²/sr)

Radiance (nW/cm²/sr)

≤ 2

> 2

District boundary

Content by: Sarp Doruk Ozturk
Map by: Sarp Doruk Ozturk, Derya Ozturk
Source: SNPP/VIIRS, Earth Observation Group

5 Discussion

RS and GIS are essential for tracking spatial and temporal patterns of light emissions (Butt 2012). Using SNPP/VIIRS DNB satellite data from 2012 to 2024 and spatial analysis methods, this study evaluated light emission trends in Samsun. The results reflect urbanization, economic growth, and infrastructure expansion, supporting previous research on the value of satellite-derived NTL data for socio-economic monitoring (Levin and Zhang 2017; Hu et al. 2018).

In 2012, most districts had low or very low emissions, indicating early urban development. By 2024, the central and coastal districts of Atakum, Ilkadim, Canik, and Tekkekoy showed substantial increases during the period from 2012 to 2018. Atakum, characterized by high population density, exhibited a stable and significant increase in light emissions, primarily due to rapid population growth driven by coastal attractiveness, expansion of residential areas, increased commercial activity, industrial growth, and infrastructure development. Similar trends were reported by Yerli et al. (2021), indicating a general increase in light emissions across Samsun. Higher emissions were primarily concentrated in coastal areas, aligning with findings from SQM measurements on light pollution in Atakum by Türk and Yavuz (2023). Although direct validation with ground-based SQM measurements or high-resolution airborne imagery was not conducted in this study due to data availability and logistical limitations, the correspondence of observed trends with these independent measurements suggests that the RS-derived NTL data reasonably reflect actual light emissions. The observed increase in light intensity also reflects urban sprawl, as noted by Ozturk (2017), highlighting a shift toward human-centered land use at the expense of natural areas. Ilkadim's port and economic base contributed to high values, while Tekkekoy and Canik grew due to industrialization and urban sprawl. These findings are consistent with studies by Cheon and Kim (2020) in Seoul, South Korea, which linked major increases in light emissions to urbanization, commercial growth, and industrialization. Growth slowed post-2018 in major districts, likely due to COVID-19 impacts and energy-saving policies. Similarly, Bustamante-Calabria et al. (2021) demonstrated that post-pandemic economic downturns in Granada, Spain, directly impacted light emissions. Meanwhile, moderate increases in light emissions were seen in Bafra, Carsamba, Terme, and 19 Mayis between 2012 and 2024, tied to trade and local industry. Rural districts (e.g., Asarcik, Ayvacik, and Yakakent) remained largely stable, consistent with the findings of Massetti (2020).

Atakum, hosting an observatory, saw »Lowest« emission areas fall from 39.0% to 2.3%, while »Medium« and »High« zones rose from 6.1% to 9.7%, threatening night sky visibility, as shown in Figure 7. Studies by Butt (2012) and Green et al. (2022) stress the importance of monitoring such zones to preserve sky quality. Figure 7 also highlights ecological areas, including the Kizilirmak Delta, Yesilirmak Delta, and Lake Ladik, which experienced shifts from »Lowest« to »Very low« categories. While still relatively dark, increasing emissions in adjacent areas indicate rising pressure from nearby development. Research by Jägerbrand and Bouroussis (2021) and Mayer-Pinto et al. (2022) emphasize the ecological risks of light pollution in sensitive habitats.

A strong correlation exists between light emissions, population metrics, and SEDI, suggesting NTL data are useful proxies for human activity (Levin and Zhang 2017). While correlation does not imply causation (Hu et al. 2018), the relationship underscores the need for integrating light pollution management into urban planning.

This study highlights the utility of RS and spatial techniques in light pollution monitoring. SNPP/VIIRS provides consistent, wide-scale data with improved radiometric quality. However, spatial resolution remains a limitation (Levin and Zhang 2017), and the lack of information on the structure of outdoor lighting (e.g., unobscured, semi-obscured, fully obscured), shielding, power, and spectral characteristics further constrains the analysis. The widespread introduction of white LED technology in urban areas has substantially altered the spectral composition of emissions and their spatial distribution. Due to their higher proportion of blue light, these LEDs intensify atmospheric scattering and amplify light pollution effects, particularly skyglow. Since SNPP/VIIRS sensors are insensitive to the extreme blue range, this spectral shift cannot be fully captured, which may partially explain discrepancies in observed radiance trends (Carias et al. 2021; Levin 2025). Future research incorporating higher-resolution imagery such as the Sustainable Development

Figure 7: Ecologically sensitive areas (Kizilirmak Delta, Yesilirmak Delta, and Ladik Lake) and the astronomical observatory. ► p. 85

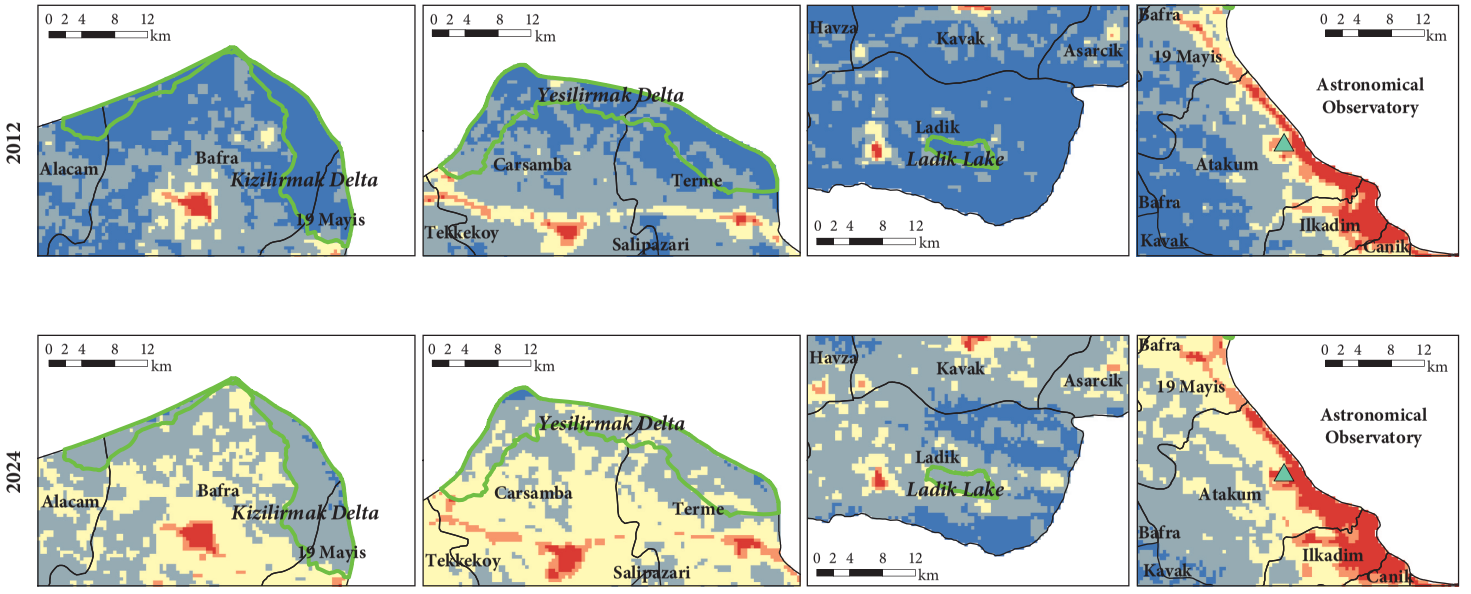

Content by: Sarp Doruk Ozturk
Map by: Sarp Doruk Ozturk, Derya Ozturk
Source: SNPP/VIIRS, Earth Observation Group

Science Satellite 1 – SDGSAT-1/GIU (Xie et al. 2024), ground-based inventories, and spectral measurements would help overcome these limitations, thereby enhancing the precision and robustness of urban light pollution assessments and enabling finer-scale planning and conservation efforts.

6 Conclusion

This study underscores the effectiveness of integrating RS and GIS techniques by advancing the application of spatial statistical and algebraic methods to identify light pollution patterns at sub-city scales. Utilizing SNPP/VIIRS DNB data spanning 2012 to 2024, the study assessed district-level changes in light pollution in Samsun. Results show a steady rise in artificial lighting, especially in coastal and central districts. Industrial zones, transport corridors, and urban sprawl contributed significantly to this increase. Areas with »Lowest« emissions declined, while »Low« and »Very low« zones expanded, reflecting a widespread diffusion of artificial light.

Light intensity correlated strongly with population, population density, and SEDI. Districts with high urban and economic activity, such as Atakum, Ilkadim, Canik, and Tekkekoy, showed the most significant increases in light pollution. Rural and agricultural districts remained less affected.

The loss of dark zones raises critical concerns regarding environmental sustainability. Atakum's observatory and natural areas like the Kizilirmak and Yesilirmak Deltas, and Lake Ladik face increasing pressure from nearby development. Immediate action is needed to protect these zones through dark sky preservation, lighting restrictions, and urban planning reforms.

The findings of this study demonstrate the significant potential of SNPP/VIIRS nighttime light data for analyzing artificial light pollution. However, future studies should incorporate higher-resolution imagery and complementary RS methodologies to assess long-term impacts and guide sustainable urban planning. The findings provide critical input for policymakers in addressing light pollution and balancing urban growth with environmental protection.

RESEARCH DATA: For information on the availability of research data related to the study, please visit the article webpage: https://doi.org/10.3986/AGS.14506.

7 References

Afify, H. A. 2011: Evaluation of change detection techniques for monitoring land-cover changes: A case study in new Burg El-Arab area. *Alexandria Engineering Journal* 50-2. https://doi.org/10.1016/j.aej.2011.06.001

Alphan, H. 2011: Comparing the utility of image algebra operations for characterizing landscape changes: The case of the Mediterranean coast. *Journal of Environmental Management* 92-11. https://doi.org/10.1016/j.jenvman.2011.07.009

Brayley, O., How, M., Wakefield, A. 2022: The biological effects of light pollution on terrestrial and marine organisms. *International Journal of Sustainable Lighting* 24-1. https://doi.org/10.26607/ijsl.v24i1.121

Bustamante-Calabria, M., Sánchez de Miguel, A., Martín-Ruiz, S., Ortiz, J. L., Vílchez, J. M., Pelegrina, A., Garcia, A. et al. 2021: Effects of the COVID-19 lockdown on urban light emissions: Ground and satellite comparison. *Remote Sensing* 13-2. https://doi.org/10.3390/rs13020258

Butt, M. J. 2012: Estimation of light pollution using satellite remote sensing and geographic information system techniques. *GIScience & Remote Sensing* 49-4. https://doi.org/10.2747/1548-1603.49.4.609

Carias, M., Fujioka, S., Phaneuf, J., Potter, M., Vaiciunas, I., Wilder, L., Wood, C., Yu, J. 2021: Preserving the night sky: Monitoring light pollution affecting the Central Idaho Dark Sky Reserve. *Technical report*. University of California.

Cheon, S., Kim, J. A. 2020: Quantifying the influence of urban sources on night light emissions. *Landscape and Urban Planning* 204. https://doi.org/10.1016/j.landurbplan.2020.103936

Chepesiuk, R. 2009: Missing the dark: Health effects of light pollution. *Environmental Health Perspectives* 117-1. https://doi.org/10.1289/ehp.117-a20

Close, O., Petit, S., Beaumont, B., Hallot, E. 2021: Evaluating the potentiality of Sentinel-2 for change detection analysis associated with LULUCF in Wallonia, Belgium. *Land* 10-1. https://doi.org/10.3390/land10010055

Cox, D. T. C., de Miguel, A. S., Bennie, J., Dzurjak, S. A., Gaston, K. J. 2022: Majority of artificially lit Earth surface associated with the non-urban population. *Science of the Total Environment* 841. https://doi.org/10.1016/j.scitotenv.2022.156782

Dong, B., Zhang, R., Li, S., Ye, Y., Huang, C. 2025: A meta-analysis for the nighttime light remote sensing data applied in urban research: Key topics, hotspot study areas and new trends. *Science of Remote Sensing* 11. https://doi.org/10.1016/j.srs.2024.100186

Earth Data, NASA 2025: VNP46A2 - VIIRS/NPP gap-filled lunar BRDF-adjusted nighttime lights daily L3 global 500m linear lat lon grid. *Dataset*. https://doi.org/10.5067/VIIRS/VNP46A2.002

Earth Observation Group, Colorado School of Mines 2025: Monthly cloud-free DNB composite. *Dataset*.

Eken, G., Bozdoğan, M., İsfendiyaroğlu, S., Kılıç, D. T., Lise, Y. (eds.) 2006: Türkiye'nin önemli doğa alanları. Doğa Derneği.

Faid, M. S., Shariff, N. N. M., Hamidi, Z. S., Wahab, R. A., Ahmad, N., Mohd Nawawi, M. S. A., Nahwandi, M. S. 2024: Alteration of twilight sky brightness profile by light pollution. *Scientific Reports* 14. https://doi.org/10.1038/s41598-024-76550-3

Forster, M. 2000: Review of the use of Geographical Information Systems in the marketing and planning of logistics services. *Christian Salvesen Logistics Research Paper* 3.

Gaston, K. J., Gardner, A. S., Cox, D. T. 2023: Anthropogenic changes to the nighttime environment. *Bioscience* 73-4. https://doi.org/10.1093/biosci/biad017

General Directorate of Protection of Natural Assets 2019: Samsun Kızılırmak Deltası doğal sit alanları sulak alan ve kuş cenneti: 2019–2023 yönetim planı. *Technical report*.

General Directorate of Water Management 2024: Yeşilırmak Havzası taşkın yönetim planı revizyon projesi. *Technical report*.

Goswami, A., Sharma, D., Mathuku, H., Gangadharan, S. M. P., Yadav, C. S., Sahu, S. K., Pradhan, M. K. et al. 2022: Change detection in remote sensing image data comparing algebraic and machine learning methods. *Electronics* 11- 3. https://doi.org/10.3390/electronics11030431

Green, R. F., Luginbuhl, C. B., Wainscoat, R. J., Duriscoe, D. 2022: The growing threat of light pollution to ground-based observatories. *The Astronomy and Astrophysics Review* 30. https://doi.org/10.1007/s00159-021-00138-3

Guk, E., Levin, N. 2020: Analyzing spatial variability in night-time lights using a high spatial resolution color Jilin-1 image–Jerusalem as a case study. *ISPRS Journal of Photogrammetry and Remote sensing* 163. https://doi.org/10.1016/j.isprsjprs.2020.02.016

Hale, J., Arlettaz, R. 2019: Artificial lighting and biodiversity in Switzerland. *Technical report*. University of Bern.

Hale, J., Blumenstein, C., Carannante, D., Arlettaz, R. 2018: Ecological light pollution in the Naturpark Gantrisch. *Technical report*. University of Bern.

Hu, Z., Hu, H., Huang, Y. 2018: Association between nighttime artificial light pollution and sea turtle nest density along Florida coast: A geospatial study using VIIRS remote sensing data. *Environmental Pollution* 239. https://doi.org/10.1016/j.envpol.2018.04.021

Hügli, F. 2021: Light pollution in European protected areas – Spatial variation of light pollution in Natura 2000 sites of the Member States of the European Union. *Master's thesis*. Eidgenössische Technische Hochschule Zürich.

Jägerbrand, A. K., Bouroussis, C. A. 2021: Ecological impact of artificial light at night: Effective strategies and measures to deal with protected species and habitats. *Sustainability* 13-11. https://doi.org/10.3390/su13115991

Ji, M., Xu, Y., Yan, Y., Zhu, S. 2024: Evaluation of the light pollution in the nature reserves of China based on NPP/VIIRS nighttime light data. *International Journal of Digital Earth* 17-1. https://doi.org/10.1080/17538947.2024.2347442

Kankanhalli, M. S., Jiang, X., Wu, J. K. 1995: A spatial algebra for content-based retrieval. In: Proceedings of the 2nd Asian Conference on Computer Vision (ACCV 1995). Nanyang Technological University.

Levin, N. 2017: The impact of seasonal changes on observed nighttime brightness from 2014 to 2015 monthly VIIRS DNB composites. *Remote Sensing of Environment* 193. https://doi.org/10.1016/j.rse.2017.03.003

Levin, N. 2023: Quantifying the variability of ground light sources and their relationships with spaceborne observations of night lights using multidirectional and multispectral measurements. *Sensors* 23-19. https://doi.org/10.3390/s23198237

Levin, N. 2025: Challenges in remote sensing of night lights – a research agenda for the next decade. *Remote Sensing of Environment* 328. https://doi.org/10.1016/j.rse.2025.114869

Levin, N., Zhang, Q. 2017: A global analysis of factors controlling VIIRS nighttime light levels from densely populated areas. *Remote Sensing of Environment* 190. https://doi.org/10.1016/j.rse.2017.01.006

Li, Y., Onasch, C. M., Guo, Y. 2008: GIS-based detection of grain boundaries. *Journal of Structural Geology* 30-4. https://doi.org/10.1016/j.jsg.2007.12.007

Li, Z., Zhao, R. L., Chen, J. 2002: A Voronoi-based spatial algebra for spatial relations. *Progress in Natural Science* 12-7.

Liu, S., Zhou, Y., Wang, F., Wang, S., Wang, Z., Wang, Y., Qin, G. et al. 2024: Lighting characteristics of public space in urban functional areas based on SDGSAT-1 glimmer imagery: A case study in Beijing, China. *Remote Sensing of Environmen*t 306. https://doi.org/10.1016/j.rse.2024.114137

Lowenthal, J., Walker, C., Benvenuti, P. 2022: Dark and quiet skies II working group reports. *Technical report*. Smith College.

Ma, J., Guo, J., Ahmad, S., Li, Z., Hong, J. 2020: Constructing a new inter-calibration method for DMSP-OLS and NPP-VIIRS nighttime light. *Remote Sensing* 12-6. https://doi.org/10.3390/rs12060937

Mander, S., Alam, F., Lovreglio, R., Ooi, M. 2023: How to measure light pollution – A systematic review of methods and applications. *Sustainable Cities and Society* 92. https://doi.org/10.1016/j.scs.2023.104465

Martinez, J. F., MacManus, K., Stokes, E. C., Wang, Z., de Sherbinin, A. 2023: Suitability of NASA's black marble daily nighttime lights for population studies at varying spatial and temporal scales. *Remote Sensing* 15-10. https://doi.org/10.3390/rs15102611

Massetti, L. 2020: Drivers of artificial light at night variability in urban, rural and remote areas. *Journal of Quantitative Spectroscopy and Radiative Transfer* 255. https://doi.org/10.1016/j.jqsrt.2020.107250

Mayer-Pinto, M., Jones, T. M., Swearer, S. E., Robert, K. A., Bolton, D., Aulsebrook, A. E., Dafforn, K. A. et al. 2022: Light pollution: A landscape-scale issue requiring cross-realm consideration. *UCL Open Environment* 4. https://doi.org/10.14324/111.444/ucloe.000036

Miller, S. D., Straka III, W., Mills, S. P., Elvidge, C. D., Lee, T. F., Solbrig, J., Walther, A. et al. 2013: Illuminating the capabilities of the Suomi National Polar-Orbiting Partnership (NPP) Visible Infrared Imaging Radiometer Suite (VIIRS) day/night band. *Remote Sensing* 5-12. https://doi.org/10.3390/rs5126717

Nobre, A., Pacheco, M., Jorge, R., Lopes, M. F. P., Gato, L. M. C. 2009: Geo-spatial multi-criteria analysis for wave energy conversion system deployment. *Renewable Energy* 34-1. https://doi.org/10.1016/j.renene.2008.03.002

Nurbandi, W., Yusuf, F. R., Prasetya, R., Afrizal, M. D. 2016: Using Visible Infrared Imaging Radiometer Suite (VIIRS) imagery to identify and analyze light pollution. *IOP Conference Series: Earth and Environmental Science* 47. https://doi.org/10.1088/1755-1315/47/1/012040

Ozturk, D. 2017: Assessment of urban sprawl using Shannon's entropy and fractal analysis: A case study of Atakum, Ilkadim and Canik (Samsun, Turkey). *Journal of Environmental Engineering and Landscape Management* 25-3. https://doi.org/10.3846/16486897.2016.1233881

Öztürk, D., Gündüz, U. 2019: Samsun ili arazi kullanımı/örtüsünün mekansal-zamansal değişimlerinin fraktal analiz kullanılarak belirlenmesi. *Uludağ Üniversitesi Mühendislik Fakültesi Dergisi* 24-2. https://doi.org/10.17482/uumfd.553486

Ozturk, D., Kilic, F. 2016: Geostatistical approach for spatial interpolation of meteorological data. *Anais da Academia Brasileira de Ciências* 88-4. https://doi.org/10.1590/0001-3765201620150103

Pan, W., Du, J. 2021: Impacts of urban morphological characteristics on nocturnal outdoor lighting environment in cities: An empirical investigation in Shenzhen. *Building and Environment* 192. https://doi.org/10.1016/j.buildenv.2021.107587

Profillidis, V. A., Botzoris, G. N. 2018: Statistical methods for transport demand modeling. In: Modeling of Transport Demand: Analyzing, Calculating, and Forecasting Transport Demand. Elsevier. https://doi.org/10.1016/B978-0-12-811513-8.00005-4

Samsun Chamber of Commerce and Industry 2022: Samsun iktisadi rapor 2022. *Technical report*.

Samsun Metropolitan Municipality 2019: Samsun ili sürdürülebilir enerji eylem planı. *Technical report*.

Song, M., Li, W., Zhou, B., Lei, T. 2016: Spatiotemporal data representation and its effect on the performance of spatial analysis in a cyberinfrastructure environment – A case study with raster zonal analysis. *Computers & Geosciences* 87. https://doi.org/10.1016/j.cageo.2015.11.005

Tenneson, K., Dilger, J., Wespestad, C., Zutta, B., Nicolau, A. P., Dyson, K., Paz, P. 2023: Change detection. In: Cloud-based Remote Sensing with Google Earth Engine: Fundamentals and Applications. Springer. https://doi.org/10.1007/978-3-031-26588-4_16

Tong, J. C., Lau, E. S., Hui, M. C., Kwong, E., White, M. E., Lau, A. P. 2022: Light pollution spatial impact assessment in Hong Kong: Measurement and numerical modelling on commercial lights at street level. *Science of The Total Environment* 837. https://doi.org/10.1016/j.scitotenv.2022.155681

Türk, Ö., Yavuz, M. 2023: Atakum ilçesinde insansız hava aracı ile ışık kirliliği ölçümleri ve değerlendirilmesi. *Süleyman Demirel University Faculty of Arts and Science Journal of Science* 18-2. https://doi.org/10.29233/sdufeffd.1221514

Unwin, D. J. 2009: Statistics, spatial. In: International Encyclopedia of Human Geography. Elsevier. https://doi.org/10.1016/B978-008044910-4.00539-3

Wang, Y., Huang, H., Wu, B. 2024: Evaluating the Potential of SDGSAT-1 Glimmer Imagery for urban road detection. *IEEE Journal of Selected Topics in Applied Earth Observations and Remote Sensin*g 18. https://doi.org/10.1109/JSTARS.2024.3502218

Widmer, K., Beloconi, A., Marnane, I., Vounatsou, P. 2022: Review and assessment of available information on light pollution in Europe. *Report*. European Environment Agency, European Topic Centre Human health and the environment.

Winsemius, S., Braaten, J. 2023: Zonal statistics. In: Cloud-based remote sensing with Google Earth Engine: Fundamentals and applications. Springer.

Wu, K., Wang, X. 2019: Aligning pixel values of DMSP and VIIRS nighttime light images to evaluate urban dynamics. *Remote Sensing* 11-12. https://doi.org/10.3390/rs11121463

Xie, Q., Cai, C., Jiang, Y., Zhang, H., Wu, Z., Xu, J. 2024: Investigating the performance of SDGSAT-1/GIU and NPP/VIIRS nighttime light data in representing nighttime vitality and its relationship with the built environment: A comparative study in Shanghai, China. *Ecological Indicators* 160. https://doi.org/10.1016/j.ecolind.2024.111945

Xu, J. 2020: Developments in management science in engineering 2018: Perspectives from scientific journals. Cambridge Scholars Publishing.

Yerli, S. K., Aksaker, N., Bayazit, M., Kurt, Z., Aktay, A., Erdoğan, M. A. 2021: The temporal analysis of light pollution in Turkey using VIIRS data. *Astrophysics and Space Science* 366-4. https://doi.org/10.1007/s10509-021-03942-6

Yin, Z., Chen, F., Dou, C., Wu, M., Niu, Z., Wang, L., Xu, S. 2024: Identification of illumination source types using nighttime light images from SDGSAT-1. *International Journal of Digital Earth* 17-1. https://doi.org/10.1080/17538947.2023.2297013